Int. J. Electrochem. Sci., 7 **(2012)** 1580 - 1601

International Journal of
ELECTROCHEMICAL
SCIENCE
www.electrochemsci.org

Investigation of Novel Heterocyclic Compounds as Inhibitors of Al-3Mg Alloy Corrosion in Hydrochloric Acid Solutions

Jasna Halambek[*]*, Marijana Jukić, Katarina Berković, Jasna Vorkapić-Furač*

Faculty of Food Technology and Biotechnology, University of Zagreb, Pierottijeva 6, 10000 Zagreb, Croatia
[*]E-mail: jhalambe@pbf.hr

Received: 16 December 2011 / *Accepted:* 13 January 2012 / *Published:* 1 February 2012

The inhibition of Al-3Mg alloy corrosion in 0.5 M and 1 M HCl by newly prepared compounds namely: 4-(methoxymethyl)-1,6-dimethyl-2-oxo-1,2- dihydropyridine-3-carbonitrile (compound A) and 4-amino-3,5-bis[6-(methoxymethyl)-3,4-dimethyl-2-oxo-1,2-dihydropyridine-1-yl]-1,2,4-triazole-2(*H*) (compound B) has been studied by weight loss and potentiodynamic polarization measurements. Tafel curves showed that both compounds investigated are excellent mixed type inhibitor for Al-3Mg alloy in acidic solutions. The adsorption of these compounds obeyed the Langmuir adsorption isotherm. FTIR analysis was used to obtain information on bonding mechanism between the metallic surface and the inhibitors. The triazole derivative (compound B) is better inhibitor than pyridine derivative (compound A).

Keywords: Acid corrosion, Aluminium alloy, Pyridine derivative, Polarization, Triazole derivative.

1. INTRODUCTION

Acids are widely used in many industries. Some important applications are industrial acid cleaning, acid pickling and acid descaling [1]. Therefore, it is very important to add an inhibitor into acidic solutions to decrease the rate of aluminium dissolution. The development of acid corrosion inhibitors based on organic compounds containing nitrogen, sulphur and oxygen atoms is the growing field of interest of corrosion and industrial chemistry [2-5]. The efficiency of these inhibitors depends not only on the characteristics of the environment in which it acts, and the nature of the metal surface and electrochemical potential at the interface, but also on the structure of the inhibitor itself. This includes the number of adsorption active centres in the molecule, their charge density, the molecular size, the mode of adsorption, the formation of metallic complexes and the projected area of the inhibitor on the metal surface [6-8]. It has been reported that N-containing inhibitors exert their best

efficiencies in hydrochloric acid [9]. Survey of literature reveals that pyridine compounds are effective corrosion inhibitors [10,11]. Furthermore, pyridine and its derivatives have been studied as corrosion inhibitors of the aluminium, and comparative studies on inhibition efficiencies of pyridine derivatives on aluminium surface have been reported previously [12,13]. Among the various nitrogenous compounds being studied as inhibitors, triazoles have been considered as environmentally acceptable chemicals [14]. Many substituted triazole compounds have been recently studied in details as effective corrosion inhibitors, mainly for steel in acidic media [15-17]. Some triazole and thiazole derivatives were studied as corrosion inhibitors for AA2024 aluminium alloy, too [18].

The goal of this research was to investigate the corrosion of Al-3Mg alloy in 0.5 M and 1 M HCl solutions in the presence of novel pyridine and triazole derivatives namely: 4-(methoxymethyl)-6-methyl-2-oxo-1,2-dihydropyridine-3-carbonitrile (compound A) and 4-amino-3,5-bis[6-(methoxymethyl)-3,4-dimethyl-2-oxo-1,2-dyhydropyridine-1-yl]-1,2,4-triazole-2(*H*) (compound B). They contain reactive centers such as nitrogen atoms with lone electrons pair and aromatic rings with delocalized π electron systems which can aid their adsorption onto metal surface. To evaluate the inhibition efficiency of these compounds in 0.5 M and 1 M HCl solutions, weight loss and potentiodynamic polarization measurements were performed. The effect of concentration and temperature on the inhibition efficiency has been examined. Meanwhile, FTIR was used to identify if there was adsorption and to provide new bonding information of the adsorption process. The surface, after treatment in the absence and in the presence of inhibitor, was analysed by scanning electron microscopy (SEM). A probable inhibitive mechanism is presented to explain the results.

2. EXPERIMENTAL

2.1. Synthesis

2.1.1. Measurements and equipments

All reactions were performed with commercially available reagents and they were used without further purification. Solvents were dried by standard methods and stored over molecular sieves (4A). All reactions were monitored by thin-layer chromatography (TLC) carried out on Merck, DC-Alufolien Kieselgel 60 F254, and detection of the components was made by short and long UV light. Products were purified by preparative thin layer chromatography on silica gel (Merck, Kieselgel 60 HF254) using the mixture dichloromethane: methanol (10:1, v/v). The solvents were of spectroscopic grade. The chemical structure and the purity of the compounds were confirmed by melting points, IR, ^{1}H- and ^{13}C-NMR spectra. The melting points were determined using an electrothermal Büchi apparatus and are not corrected. The IR spectra were recorded in CH_2Cl_2 solution with a Bomem MB 100 mid IR spectrophotometer. The ^{1}H- and ^{13}C-NMR spectra were recorded on a Bruker Avance 300 or Bruker Avance 600 MHz spectrometer in DMSO-d_6 solution with $(CH_3)_4Si$ as internal standard.

The microwave-assisted reactions were performed using a controllable single-mode microwave reactor, Start S (Milestone) Microwave Labstation for Synthesis. The reactor is equipped with a magnetic stirrer as well as a temperature and power controls.

Compound 4 - (methoxymethyl) - 1,6 – dimethyl - 2-oxo - 1, 2 – dihydropyridine-3-carbonitrile (compound A) was synthesized according to the laboratory procedures reported previously [19,20].

The synthesis of the compound B was performed according to the Scheme 1.

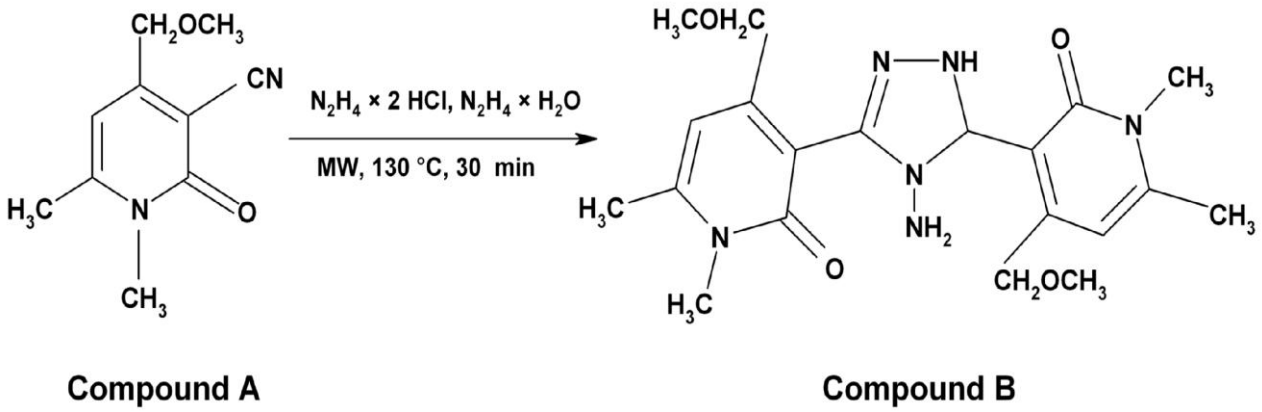

Scheme 1. Synthesis of 4-amino-3,5-bis[6-(methoxymethyl)-3,4-dimethyl-2-oxo-1,2 dihydropyridine-1-yl]-1,2,4-triazole-2(*H*) (compound B)

2.1.2. Synthesis of 4-amino-3,5-bis[6-(methoxymethyl)-3,4-dimethyl-2-oxo-1,2-dihydropyridine-1-yl] 1,2,4-triazole-2(H)(compound B)

A mixture of 4-(methoxymethyl)-1,6-dimethyl-2-oxo-1,2-dihydropyridine-3- carbonitrile (compound A) (1.92 g, 0.01 mol), hydrazine dihydrochloride (2.05 g, 0.01 mol) and hydrazine hydrate (3 mL, 0.03 mol) in ethylene glycol (10 mL) was introduced into a flask placed in microwave reactor, under a reflux condenser and irradiated for 30 min (500 W) at 130 °C under magnetic stirring. After cooling, the reaction mixture was diluted with water (20 mL) and dichloromethane was used to extract the product.

The organic phase was then dried over Na_2SO_4. The orange solid obtained after evaporation of the solvent was purified by column chromatography on a silica gel as adsorbent and dichloromethane: methanol (10:1, v/v) as eluent to afford yellow solid 4-amino-3,5-bis[6-(methoxymethyl)-3,4-dimethyl-2-oxo-1,2-dihydropyridine-1-yl]-1,2,4-triazole-2(*H*) (compound B) (yield 73 %, m.p. 98-99.5 °C). Elemental analysis, calculated for $C_{20}H_{28}N_6O_4$ (416.26) : % C 57.70; % H 6.72; % N 20.19; Found: % C 57.36; % H 6.18; % N 19.81; ^{1}H-NMR (DMSO-d_6) δ: 9.07 (1H, s, N*H*), 6.59 (1H, s, C*H*), 6.38 (2H, s, NH_2), 4,87 (2H, s, C*H*), 4.48 (4H, s, CH_2O), 3.57,3.56 (6H, d, N–CH_3), 3.49, 3.45 (6H, d, OCH_3), 2.46, 244 (6H, d, CH_3) ppm. ^{13}C-NMR (DMSO-d_6) δ: 163.32, 159.48 (*C*=O,C-2′), 157.88 (*C*H–C-3), 153.02 (*C*–5), 152.91, 152.23 (*C*–4′), 115.88, 114.43 (*C*–3′), 105.14, 105.27 (*C*H,*C*–5′), 72.53, 70.81 (*C*H_2O), 59.11, 58.97 (O*C*H_3), 31.80, 31.50 (N–*C*H_3), 21.75, 21.53 (*C*H_3) ppm.

2.2. Weight loss measurements

Corrosion tests were performed using coupons prepared from Al-3Mg alloy. The chemical composition (wt %) of the Al-3Mg alloy sample is Mg 3.10, Si 0.40, Fe 0.40, Cu 0.10, Mn 0.50, Cr 0.30, Zn 0.20, Ti 0.15 and balanced Al.

Each sheet was 0.15 cm in thickness and was mechanically press-cut into coupons of dimension 2 cm × 2 cm. All the surfaces of the specimens were abraded successively with fine grade emery papers (600, 800 and 1200 grids), then the metal surface was rinsed with distilled water, ultrasonically degreased in absolute ethanol, dried in acetone and stored in moisture-free desiccators prior to use.

The aggressive acid solutions were made from analytical grade hydrochloric acid (HCl). Appropriate concentrations of acid (0.5 M and 1 M) were prepared by using deionised water and used in absence and presence of certain inhibitor concentration (1×10^{-6} to 1×10^{-3} M).

In each experiment, the cleaned aluminium coupon was weighed and suspended with the aid of glass rod and hook in a beaker containing 150 mL test solution. The temperature was controlled using a thermostat.

All the aggressive acid solutions were open to air. The immersion time for the weight loss test was 3 h at 25 °C, 40 °C, 60 °C and 80 °C in non-de-aerated test solutions. The coupon was then taken out from the test solution, washed with distilled water, dried and re-weighed.

The corrosion rate (W) and the inhibition efficiency η_w (%) were calculated from equations (1) and (2):

$$W = \frac{\Delta m}{S \cdot t} \qquad (1)$$

$$\eta_w(\%) = \left(\frac{W'_{\text{corr}} - W_{\text{corr}}}{W'_{\text{corr}}} \right) \times 100 \qquad (2)$$

where Δm is average weight loss of three parallel Al-3Mg alloy sheets (mg), S the total area of the specimen (cm^2), t is immersion time (h), W_{corr} and W'_{corr} are the corrosion rates of Al-3Mg samples with and without inhibitor, respectively.

The inhibition efficiency depends on the degree of coverage of the Al-3Mg alloy surface by molecules of the inhibitor and can be expressed as in the following equation:

$$\theta = \frac{W'_{\text{corr}} - W_{\text{corr}}}{W'_{corr}} \qquad (3)$$

where θ is the surface coverage.

2.3. Potentiodynamic polarization measurements

Potentiodynamic polarization measurements were carried out in a conventional three electrode cylindrical glass cell containing 600 mL of electrolyte with and without inhibitor. A saturated calomel electrode (SCE) and graphite electrode were used as reference and auxiliary electrodes, respectively. The working electrode (WE) cut from Al-3Mg alloy was mounted in Teflon holder so that exactly of

1 cm^2 area was exposed to corrosive solution. In order to minimize ohmic contribution, the Luggin capillary was placed close to the working electrode. Before measurements the working electrode was abraded successively on test face with fine grade emery papers (600, 800 and 1200 grids), then the metal surface was rinsed with distilled water, ultrasonically degreased in absolute ethanol, dried in acetone and finally dipped in the electrolytic cell. Each experiment was repeated at least three times to check the reproducibility. The electrochemical measurements were performed in the test solution after reaching the open-circuit potential (E_{ocp}).

The polarization curves were recorded with a potentiostat type VersaSTAT 3 (Princeton Applied Research), at scan rate of 0.5 mV s^{-1}. The temperature was thermostatically controlled at (25±0.1) °C. Before measurements the test solution was deaerated for 30 min in the cell with pure nitrogen to avoid oxygen influence on metal surface. All reported potentials refer to SCE.

In the case of electrochemical measurements, equation (4) was used to determine the inhibition efficiency:

$$\eta_P(\%) = \left(\frac{I'_{corr} - I_{corr}}{I'_{corr}} \right) \times 100 \qquad (4)$$

where I'_{corr} and I_{corr} are the corrosion current densities in the absence and presence of inhibitor to be determined by the intersection of the extrapolated cathodic Tafel lines at the experimentally measured open-circuit potential, and corrosion potential (E_{corr}), respectively.

The polarization resistance, R_p, was determined from the slope of polarization curves obtained on the basis of measurements in the potential range ±20 mV from the corrosion potential with scanning rate of 0.25 mV s^{-1}. However, the polarization curves are not completely linear in this potential domain, thus, the polarization resistance was determined from the experimental data collected in ±5 mV around the corrosion potential.

2.4. Fourier transform infrared (FTIR) spectra

The interaction between the organic molecules and the metal surface has been studied by means of FTIR reflection spectra. Fourier transform infrared (FTIR) spectra were recorded with spectrometer Spectrum 100, PerkinElmer using attenuated total reflectance (ATR) technique. ATR-FTIR spectra of pure compounds A and B were compared with spectra recorded on the surface products deposited on the test coupons after 3 h exposure at room temperature in 1 M HCl solutions with optimum concentrations of compound A and B ($c = 1\times10^{-4}$ M).

2.5. SEM examination

Scanning electron microscopy (SEM) was used to study the surface morphology of the Al-3Mg alloy. The surface morphology of the samples, after 3 h immersion in 1 M HCl solutions in absence and presence of compounds studied (c = 1×10^{-4} M), was performed on JEOL JSM-6460 scanning electron microscope.

3. RESULTS AND DISCUSSION

3.1. Synthesis

Compound B (4-amino-3,5-bis[6-(methoxymethyl)-3,4-dimethyl-2-oxo-1,2-dihydropyridine-1-yl]-1,2,4-triazole-2(*H*)) was synthesized by the nucleophilic attack of hydrazine derivatives on nitrile (compound A) [20,22] under microwave irradiation, using previously described synthetic method [23] with minor modifications. The same compound B was prepared under microwave irradiation by the reaction of 4-(methoxymethyl)-1,6-dimethyl-2-oxo-1,2-dihydropyridine-3-carbonitrile (compound A) with hydrazine dihydrochloride in the presence of an excess of hydrazine hydrate in ethylene glycol. Minor modifications were made in isolation and purification techniques. It was found that better yields were obtained when the reaction was performed at 130 °C for 30 min at 500 W.

3.2. Weight loss measurements

The effect of addition of compound A and compound B at different concentrations on the corrosion of Al-3Mg alloy in 0.5 M and 1 M HCl solution was studied by weight loss method at 25 °C after 3 h of immersed period.

The representative plots of weight loss against time for Al-3Mg alloy in 0.5 M HCl and 1 M HCl, respectively, in the absence and present of different concentrations of compound B at 25 °C are shown in Fig. 1a and 1b. The figures clearly show a great reduction in weight loss of the metal coupons in the presence of the inhibitor B compared to the hydrochloric solutions alone. Similar plots were obtained with the compound A, in both solutions.

The values of corrosion rate (W), surface coverage (θ) and inhibition efficiency η_w (%) obtained from weight loss method are summarized in Table 1. It is very clear that compounds investigated inhibit the corrosion of Al-3Mg alloy in 0.5 M and 1 M HCl solutions, at all concentrations used in this study, and the corrosion rate (W) decreases continuously with increasing inhibitor concentrations added at 25 °C.

The highest inhibition efficiency is related to compound B, reaching the maximum value of 89 % in 0.5 M HCl and 94 % in 1 M HCl solution for the concentration 1×10^{-4} M, while for compound A the best inhibition efficiency was obtained in 1 M HCl solution (90 %) and 84 % in 0.5 M HCl for the concentration 1×10^{-3} M, respectively.

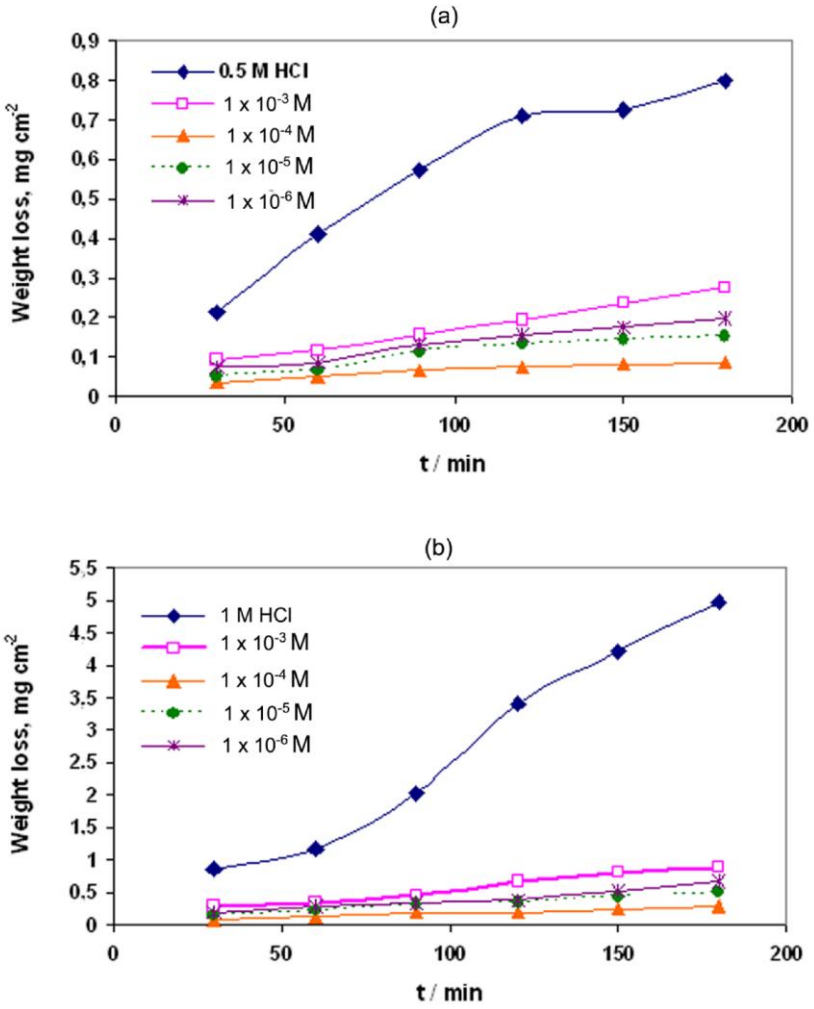

Figure 1. Weight loss vs. immersion time for Al-3Mg in (a) 0.5 M HCl and (b) 1 M HCl with various concentrations of compound B at 298 K.

Table 1. Corrosion rate, surface coverage and inhibition efficiency for Al-3Mg alloy in 0.5 M and 1 M HCl alone and in presence of different concentrations of compounds A and B at 298 K after 3 h exposure.

HCl conc.	Inhibitor conc. (M)	Compound A			Compound B		
		W (mg cm^{-2} h^{-1})	θ	η_w (%)	W (mg cm^{-2} h^{-1})	θ	η_w (%)
0.5 M	0	0.26	-	-	0.26	-	-
	1×10^{-6}	0.12	0.53	53	0.07	0.75	75
	1×10^{-5}	0.08	0.68	68	0.05	0.81	81
	1×10^{-4}	0.06	0.77	77	0.03	0.89	89
	1×10^{-3}	0.04	0.84	84	0.09	0.65	65
1 M	0	1.66	-	-	1.66	-	-
	1×10^{-6}	0.87	0.48	48	0.22	0.87	87
	1×10^{-5}	0.56	0.66	66	0.16	0.90	90
	1×10^{-4}	0.36	0.78	78	0.09	0.94	94
	1×10^{-3}	0.16	0.90	90	0.29	0.83	83

For compound B was observed that the inhibition efficiency reaching a maximum value for the concentration 1×10^{-4} M and then fall with higher concentration 1×10^{-3} M. We assume that the highest inhibitive concentration is limited by the solubility of the tested compound B. Similar observation was reported previously [24]. From the results obtained it can be concluded that triazole compound B is better inhibitor than pyridine compound A, because the variation in inhibitive efficiency mainly depends on the type and the nature of the substituents present in the inhibitor molecule. The plausible mechanism for corrosion inhibition of Al-3Mg alloy in 0.5 M and 1 M HCl by these compounds may be explained on the basis of adsorption behaviour. The high inhibitive performance of compound B suggests a higher bonding of this 1,2,4-triazole molecule to the surface, probably due to higher number of lone electron pairs from heteroatoms and π-orbitals. Also, the larger molecular size of triazole compound can be considered to ensure greater coverage of the metallic surface [24, 25]. The observed high inhibition efficiencies of compound A and compound B, apart from depending on their molecular structure, may also depend on many other factors such as the number of adsorption active centres in the molecule and their charge densities, molecular size, mode of adsorption, heat of hydrogenations, and formation of metallic complex, as well as the projected area of the inhibitor on the metal surface [2,3,26].

3.3. Polarization measurements

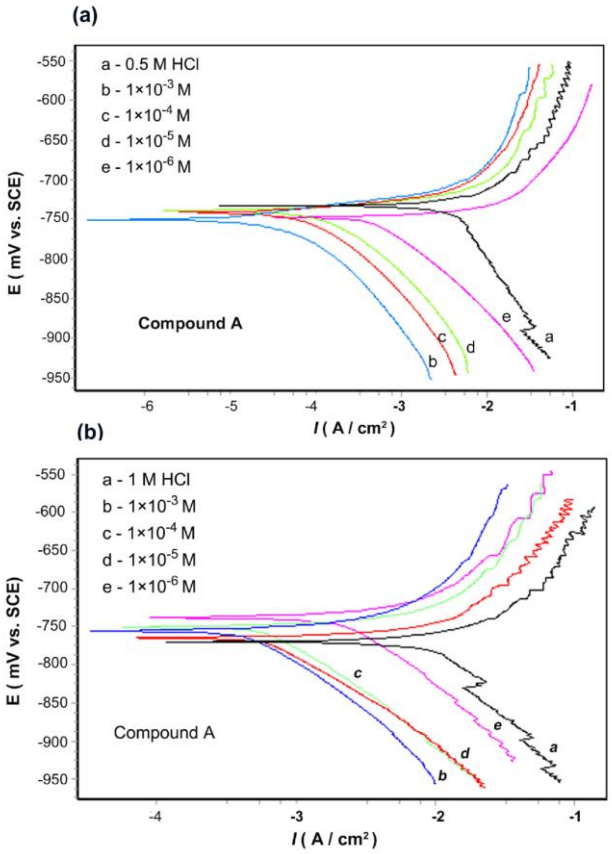

Figure 2. Potentiodynamic polarization curves obtained for Al-3Mg alloy in (a) 0.5 M HCl and (b) 1M HCl with various concentrations of compound A at 298 K.

Examples of potentiodynamic polarization curves for Al-3Mg alloy in hydrochloric acid solutions, containing various concentrations of compounds A and B, are shown in Fig. 2. and Fig. 3. It can be seen that both, the anodic and cathodic current densities obtained in 0.5 M HCl and 1 M HCl solutions in the presence of inhibitors under investigation are lower than corrosion current densities obtained in acid solutions in the absence of these compounds. In all cases, addition of the compounds studied induced a marked decrease in the cathodic and a slight decrease in the anodic current densities (especially in 0.5 M HCl solution). Accordingly, these inhibitors affected the dissolution of the metal and greatly affect the hydrogen evolution processes. Also, it is evident that compound A suppressed the anodic dissolution to greater extent than compound B.

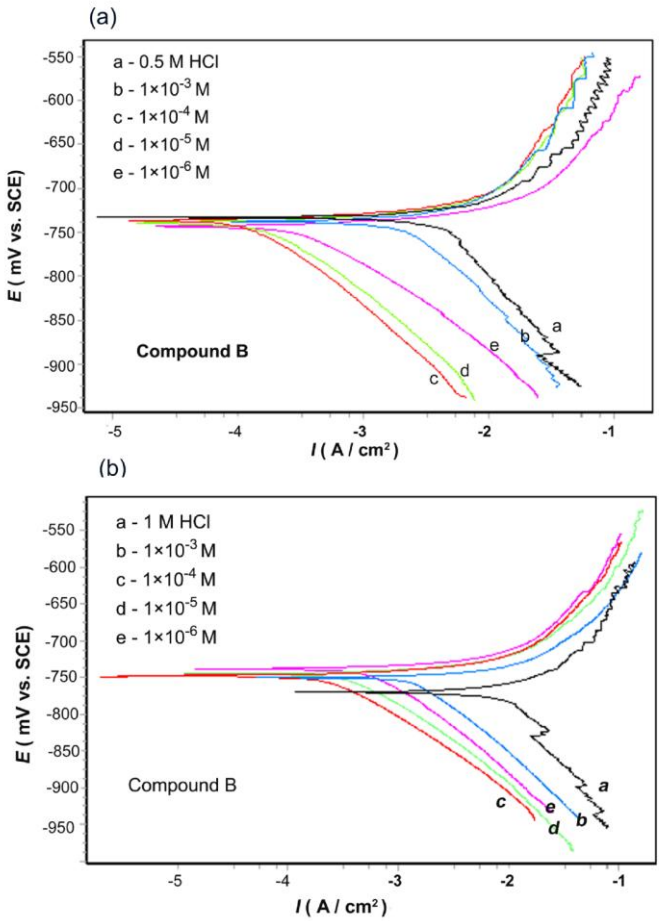

Figure 3. Potentiodynamic polarization curves for Al-3Mg alloy in (a) 0.5 M HCl and (b) 1 M HCl with various concentrations of compound B at 298 K.

Table 2. represents the electrochemical parameters (E_{corr}, I_{corr}, β_c, R_p and η_P (%)) obtained from potentiodynamic polarization and polarization resistance measurements for Al-3Mg alloy in HCl solutions in absence and presence of various concentrations of the compounds A and B at 25 °C. For compound B was noticeable the nonlinearity in concentration and current density. A lowest I_{corr} value was observed for 1×10^{-4} M concentration which showed a maximum efficiency of 97.8 % and 96.5 %

in 0.5 M and 1 M HCl solutions, respectively. For 1×10^{-3} M concentration the inhibition efficiency was found to decrease. Similar trend of decreasing the inhibition efficiency even with increase in inhibitor concentrations after achieving a maximum efficiency at critical inhibitor concentration were also reported earlier [27,28].

Corrosion potential (E_{corr}) was found to shift towards more positive direction with the increase in the inhibitor concentration in 1 M HCl solution for both compounds added. Values for cathodic Tafel slope (β_c) were found to decrease in the presence of inhibitors, indicating the influence of compounds studied on the kinetics of hydrogen evolution reaction [17]. It could be concluded that the inhibitors influence both, the cathodic and anodic reaction, of the corrosion process in 1 M HCl solution, what means that both compounds work in the present case as a mixed type inhibitor. In 0.5 M HCl solution, compounds A and B show similar electrochemical behaviour, but in this aggressive medium these compounds have greater effect on cathodic reaction. The values for E_{corr} change slightly in negative direction, while the values for cathodic Tafel slope (β_c) decrease in the presence of inhibitors indicating that the hydrogen evolution reaction is not diminished by the surface blocking effect of compounds studied [29]. Accordingly, these inhibitors affected the dissolution of the metal and the hydrogen evolution processes.

Table 2. Polarization parameters for Al-3Mg alloy in 0.5 M and 1 M HCl containing different concentrations of compounds A and B at 298 K.

System	*c* (M)	Potentiodynamic polarization				Linear polarization		
		$-E_{corr}$ (mV)	I_{corr} (mA cm^{-2})	$-\beta_c$ (mV dec^{-1})	η_P (%)	R_p (Ω cm^2)	I_{corr} (mA cm^{-2})	η_{LP} (%)
HCl	0.5	-733	6.44	131	-	2.33	6.95	-
Compound A	1×10^{-6}	-748	0.97	96	84.9	4.45	1.04	85.0
	1×10^{-5}	-739	0.41	118	93.6	19.45	0.73	89.4
	1×10^{-4}	-741	0.30	91	95.3	28.10	0.55	92.1
	1×10^{-3}	-750	0.20	115	96.8	38.55	0.32	95.3
Compound B	1×10^{-6}	-743	0.42	99	93.5	13.47	0.66	90.5
	1×10^{-5}	-739	0.22	117	96.5	32.22	0.34	95.1
	1×10^{-4}	-736	0.14	98	97.8	42.60	0.22	96.8
	1×10^{-3}	-738	2.64	94	59.1	3.36	2.05	70.5
HCl	1	-769	10.20	162	-	1.43	11.50	-
Compound A	1×10^{-6}	-738	3.66	150	64.1	5.54	3.09	73.1
	1×10^{-5}	-750	0.92	132	90.9	9.41	1.24	89.2
	1×10^{-4}	-765	0.85	117	91.6	9.54	0.86	92.5
	1×10^{-3}	-755	0.60	152	94.2	17.10	0.32	97.2
Compound B	1×10^{-6}	-738	0.71	117	93.0	9.88	1.05	90.8
	1×10^{-5}	-744	0.46	112	95.5	12.63	0.89	92.2
	1×10^{-4}	-748	0.35	106	96.5	19.08	0.62	94.6
	1×10^{-3}	-750	1.48	102	85.4	5.44	1.27	88.9

Polarization resistances, R_p for Al-3Mg alloy in hydrochloric acid solution, in the absence and presence of inhibitors, were determined from the current-potential curves in the vicinity of E_{corr} . The data are shown in Table 2. The results clearly indicate that the I_{corr} values decreased and the R_p values, as expected, increased in the presence of inhibitors, indicating that the corrosion process was suppressed following the increase in inhibitor concentration. The inspection of results in Table 2. indicates again, that compound B is better inhibitor.

It inhibits the corrosion process in the studied range of concentrations, and η_{LP} (%) increases with concentration, reaching its maximum value, 96.8 % and 94.6 % in 0.5 M and 1 M HCl, respectively, at the 1×10^{-4} M concentration. For compound A the highest inhibition efficiency reaches a maximum value of 92.5 % at optimum concentration of 1×10^{-4} M in 1 M HCl solution. A very important criterion to characterize the efficiency of inhibitors is to determine the ratio of their efficiency to concentration. High protection at low inhibitor concentration is required to maintain appropriate inhibitor concentration and to avoid insufficient inhibition, as well as for economic reasons [29]. Results obtained from polarisation studies show that the inhibition efficiency decreases in the same order as observed in gravimetric measurements.

3.4. Adsorption isotherms

Basic information on the interactions between the inhibitors and the Al-3Mg alloy surface can be provided by the adsorption isotherms, which provide information about the interaction among the adsorbed molecules themselves and their interactions with the electrode surface [30]. The fractional surface coverage θ can be easily determined from the weight loss measurements data by the ratio η_w (%) / 100, if one assumes that the values of η_w (%) do not differ substantially from θ.

When the fraction of the surface covered is determined as a function of the concentration at a constant temperature, adsorption isotherm could be evaluated at equilibrium conditions. In order to acquire a better understanding of adsorption mode of the adsorbate on the surface of the aluminium alloy samples, the data obtained from the weight loss were tested with several adsorption isotherms. Langmuir adsorption isotherm was found to fit well with the experimental data. The adsorption isotherm relationship of Langmuir is represented by the following equation (5):

$$\frac{\theta}{1-\theta} = K_{ads}c \qquad (5)$$

where c is the inhibitor concentration in mol dm^{-3}, θ the surface coverage and K_{ads} is the equilibrium constant of adsorption process. It is noted that the straight line obtained on plotting log (θ / 1- θ) vs. log c as shown in Fig. 4. suggests that the adsorption of inhibitor on Al-3Mg surface in HCl solutions follows the Langmuir's adsorption isotherm.

This isotherm postulates that there is no interaction between the adsorbed molecules, and the energy of adsorption is independent of the surface coverage. Langmuir's isotherm assumes that the solid surface contains a fixed number of adsorption sites, and each holds one adsorbed species [6].

The free energy of adsorption (ΔG^0_{ads}) was calculated from the following equation (6):

$$\Delta G^0_{ads} = -RT \ln(55.5 K_{ads}) \qquad (6)$$

where 55.5 mol dm^{-3} is the molar concentration of water in the solution, R is the gas constant and T is the absolute temperature [31] . Thermodynamic parameters for adsorption process obtained from Langmuir's adsorption isotherm for the compounds A and B are given in Table 3.

It is generally accepted [8,25], that according to the values of ΔG^0_{ads} up to -20 kJ mol^{-1}, the adsorption was regarded as physisorption, and inhibition acted due to the electrostatic interactions between the charged molecules and the charged metal. The values for ΔG^0_{ads} around -40 kJ mol^{-1} were seen as chemisorption, which is due to the charge sharing or a transfer from the inhibitor molecules to the metal surface forming a covalent bond [32].

The values of ΔG^0_{ads} in these measurements range from -39.6 kJ mol^{-1} to -41.1 kJ mol^{-1} for compound A and compound B, respectively. It is suggested that the adsorption of compounds investigated involves chemisorption process. However, some researchers have reported [33] that adsorption of inhibitor molecules is not merely physisorption or chemisorption but obeying a comprehensive adsorption (physical and chemical adsorption) for the same value. However, which kind of adsorption will play a more important role in the corrosion inhibition would be discussed further.

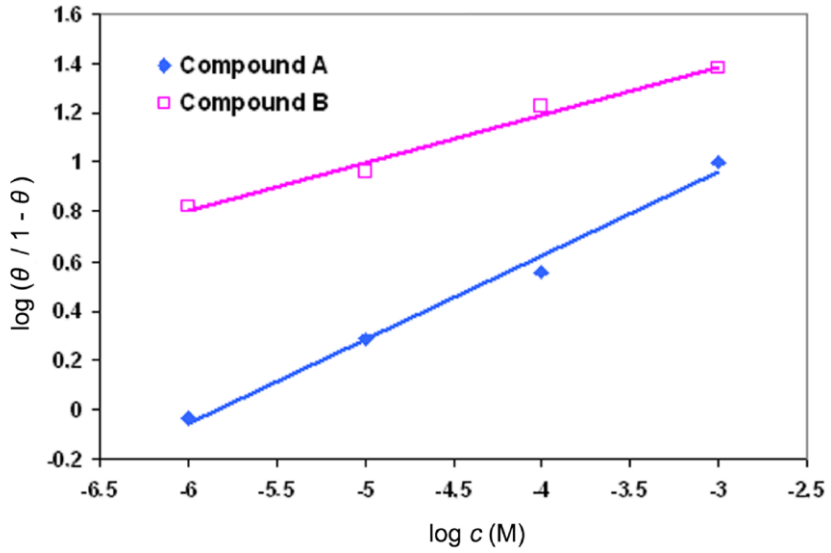

Figure 4. Langmuir's adsorption plots for Al-3Mg alloy in 1 M HCl with various concentrations of compounds studied at 298 K.

The values of K_{ads} obtained from Eq. (5) are high for both compounds studied and indicate strong adsorption on aluminium alloy surface in acidic medium. The strong interaction of inhibitor with Al-3Mg alloy surface can be attributed to the presence of nitrogen and oxygen atoms and π-electrons in the inhibitor molecules. Some authors have reported that the higher K_{ads} value (> 100 M^{-1}), the stronger and more stable adsorbed layer is forming causing the higher inhibition efficiency [34].

Table 3. Thermodynamic parameters for the adsorption of compounds A and B (c=1×10^{-4} M) in 0.5 M and 1 M HCl on the Al-3Mg alloy at 298 K.

Inhibitors	0.5 M HCl		1 M HCl	
	K (10^4 M^{-1})	ΔG^0_{ads} (kJ / mol)	K (10^4 M^{-1})	ΔG^0_{ads} (kJ / mol)
A	15.6	-39.6	28.3	-41.0
B	25.5	-40.8	29.4	-41.1

3.5. Effect of temperature

To evaluate the adsorption of compounds A and B and activation parameters of the corrosion process of Al-3Mg alloy in acidic media, weight loss measurements were done in the temperature range of 298–353 K, in the absence and presence of compounds at optimum concentration 1×10^{-4} M during 3 h immersion time. The variation of inhibition efficiency with temperature is given in Fig. 5.

The effect of temperature on the inhibited acid-metal reaction is very complex. Many changes such as rapid etching desorption of inhibitor, as well as inhibitor decomposition occur on the metal surface [35]. The results revealed that, on increasing temperature, there is a decrease in inhibition efficiency for both compounds used. Generally, the metallic corrosion in acidic media is accompanied with evolution of hydrogen gas, and rise in the temperature usually accelerates the corrosion reactions resulting in higher dissolution rate of the metal [36]. A decrease in inhibitor efficiency with temperature can be attributed to the increased desorption of inhibitor molecules from the metal surface, or decreased adsorption process strength at elevated temperature suggesting a physical adsorption mode. Temperature investigations are also required, although they do not furnish all of the information needed for the elucidation of adsorption character. There are cases in which chemical adsorption is accepted, although inhibition efficiency decrease with increasing temperature [37].

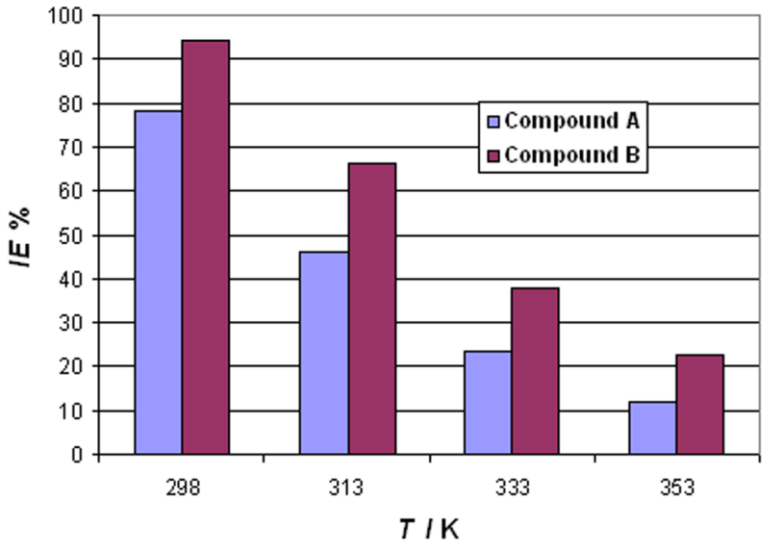

Figure 5. Inhibition efficiency of compound A and B (c = 1×10^{-4} M) in 1 M HCl at different temperatures.

The activation energy E_a for Al-3Mg dissolution in 0.5 M and 1 M HCl in the absence and presence of inhibitors were calculated from the Arrhenius equation (7):

$$\log\frac{W_2}{W_1} = \frac{E_a}{2.303R}\left(\frac{1}{T_1} - \frac{1}{T_2}\right) \qquad (7)$$

where W_1 and W_2 are corrosion rates at temperatures T_1 and T_2, respectively and E_a is the apparent activation energy for corrosion process which represents the energy necessary for a molecule to possess in order to react [38].

The value of heat of adsorption (Q_{ads}) was calculated for the trend of surface coverage with temperature according to the following equation:

$$Q_{ads} = 2.303R\left[\log\left(\frac{\theta_2}{1-\theta_2}\right) - \log\left(\frac{\theta_1}{1-\theta_1}\right)\right] \times \left(\frac{T_1 \cdot T_2}{T_2 - T_1}\right) \qquad (8)$$

where θ_1 and θ_2 are the degrees of surface coverage at temperature T_1 and T_2 [39].

The values of thermodynamic parameters for the adsorption of inhibitors can provide valuable information about the mechanism of corrosion inhibition.

The values of activation parameters for Al-3Mg alloy in HCl solutions are presented in Table 4. It can be seen that E_a values are higher in the presence of inhibitors than those in inhibitors absence. Some conclusions on the mechanism of the inhibitor action can be obtained by comparing E_a, both in the presence and absence of the corrosion inhibitor.

The higher value of the activation energy (Ea) of the process in an inhibitor's presence, when compared to that in its absence, is attributed to its physical adsorption, while chemisorption is more pronounced in the opposite case.

The relationship between the temperatures, inhibition efficiency η (%) of an inhibitor and the activation energy in the presence of an inhibitor was given as follows [40]:

(i) for inhibitor, whose η (%) decreases with temperature increase, the value of activation energy (Ea) found is greater than that in the solution without inhibitor,

(ii) for inhibitors, whose η (%) does not change with temperature variation, the activation energy (Ea) does not change in the presence or absence of inhibitors,

(iii) for inhibitors, whose η (%) increases with temperature increase, the value of activation energy (Ea) found is less than that in the solution without inhibitors.

As adsorption decreases more desorption of inhibitor molecules occurs because these two opposite processes are in equilibrium. Due to more desorption of inhibitor molecules at higher temperatures the greater surface area of aluminium alloy comes in contact with aggressive environment, resulting in an increase of corrosion rates with temperature. The increase in activation energy after the addition of the inhibitor to acid solutions can indicate that physical adsorption (electrostatic) occurs in the first stage. The results show a stronger physisorption of compound B than compound A on the electrode surface. Physical adsorption is small but important because it is

preceding stage of chemisorption of investigated organic compounds on Al-3Mg alloy surface [24]. The increase in the activation energy also indicates a strong adsorption of the inhibitor molecules on Al-3Mg alloy surface.

Table 4. Calculated values of activation energy (E_a) and heat of adsorption (Q_{ads}) for Al-3Mg alloy dissolution in acid solution in absence and presence of compounds A and B.

System	E_a (kJ mol^{-1})	Q_{ads} (kJ mol^{-1})
0.5 M HCl (blank)	33.34	-
0.5 M HCl + compound A	54.89	-34.36
0.5 M HCl + compound B	63.06	-41.51
1 M HCl (blank)	12.43	-
1 M HCl + compound A	35.56	-48.49
1 M HCl + compound B	57.18	-64.15

The negative Q_{ads} values indicate that the degree of surface coverage decreases with rise in temperature and physisorption mechanism is proposed. Of course, after these molecules are adsorbed on the aluminum surface by the electrostatic forces, they may still react with metal to form the chemical bonds. The great adsorption heat indicates this possibility, especially for compound B in 1 M HCl solution. The observed variation of activation energy with inhibition efficiency suggests that the inhibition process is controlled. Also, the thermodynamic parameters confirm that compounds investigated have effect on both, cathodic and anodic reactions, being in good correlation with results obtained by electrochemical measurements.

3.6. FTIR analysis

In this paper, FTIR spectrometer was used to evaluate the protective layer formed on the Al-3Mg alloy surface in presence of inhibitors and to provide the possible interactions between the organic molecules and the Al-3Mg alloy surface. Several researchers have confirmed that FTIR analysis is an excellent method that can be used to determine the type of bonding for organic inhibitors adsorbed on the metal surface [41-43]. Fig. 6. shows the FTIR spectra (a) of compound A and adsorbed protective layer formed on Al-3Mg surface after 3 h immersion in 1 M HCl solution with optimum concentrations of compound A (b).

The FTIR spectrum of pure compound A is shown in Fig. 6(a). The weak bands in region from 3083 to 2829 cm^{-1} are attributed to C–H stretching vibrations in aromatic ring. The absorption band at 2218 cm^{-1} is attributed to C≡N stretching vibration and the strong band at 1642 cm^{-1} to C=O. The absorption bands at 1582, 1537, 1219 and 1201 cm^{-1} are due to the framework vibrations of pyridine ring. The bands in the region from 1473 to 1363 cm^{-1} are attributed to C–H bending in $–CH_2$ and $–CH_3$, respectively. Besides these, there are absorption bands at 1114 and 1029 cm^{-1}, which can be assigned to the C–N and C–O stretching vibrations. The bands below 1000 cm^{-1} are assigned to the C–H bending vibrations.

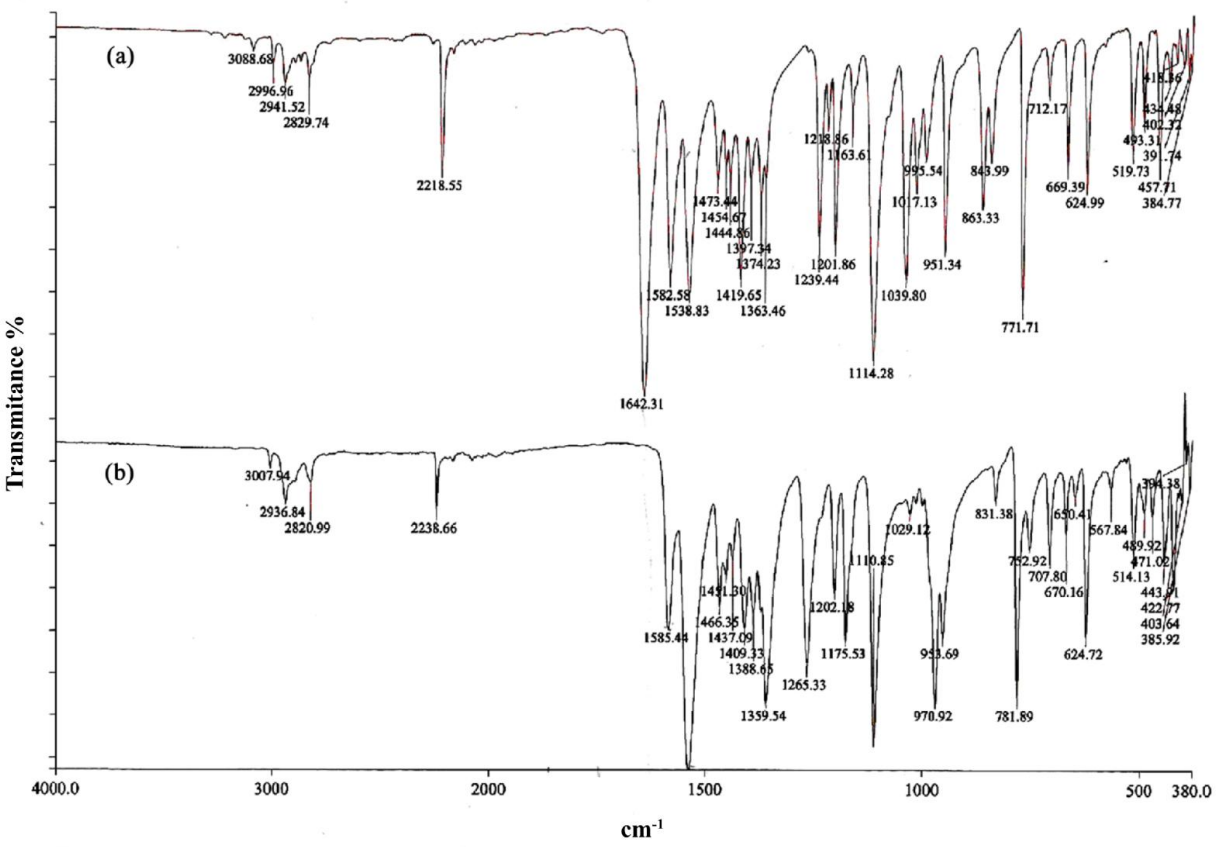

Figure 6. FTIR spectra (a) of compound A and (b) adsorption layer formed on the Al-3Mg alloy surface after immersion in 1 M HCl solution containing compound A ($c = 1\times10^{-4}$ M) for 3 h at 298 K.

The FTIR spectrum of adsorbed protective layer formed on Al-3Mg surface after 3 h immersion in 1 M HCl solution containing compound A ($c = 1\times10^{-4}$ M) is shown in Fig. 6(b). As can be seen all important peaks in pure compound appeared in adsorption layer on the Al-3Mg alloy surface except the band attributed to C=O stretching vibration. The disappearance of C=O stretching vibration from 1642 cm^{-1} and the C≡N stretching vibration at 2218 cm^{-1} shifting to higher wave number (2238 cm^{-1}) reveal the fact that compound A is adsorbed on the Al-3Mg alloy surface. The weak bands at 752 and 707 cm^{-1} which do not appear in Fig. 6(a) are assigned to asymmetrical and symmetrical Al–O bending [44]. Therefore, the new band at 567 cm^{-1} is due to Al–N stretching vibration [45]. The results could suggests the presence of a trace of the compound A complex with Al^{3+} on the surface and gives an evidence for the chemisorption of compound A on Al-3Mg alloy surface. Fig 7(a) show the FTIR spectrum of pure compound B. The absorption bands in the region from 3390 to 3223 cm^{-1} are attributed to N–H and $–NH_2$ stretching vibrations. The weak bands in region from 3088 to 2892 cm^{-1} are characteristic for C–H stretching vibration in aromatic ring. The absorption band at 1640 cm^{-1} is attributed to C=O stretching vibration, while bands in the region from 1580 to 1531 cm^{-1} are attributed to C=C bending vibrations in pyridine ring. The bands in the region from1471 to 1363 cm^{-1} are attributed to C–H bending in $–CH_2$ and $–CH_3$, respectively. The absorption bands in the area 1298 – 1113 cm^{-1} can be assigned to the C–N and C–O stretching vibrations. In the

area below 1000 cm^{-1} bands appear due to the bending vibrations "out of the plane" and their position is determined by the position of substituents.

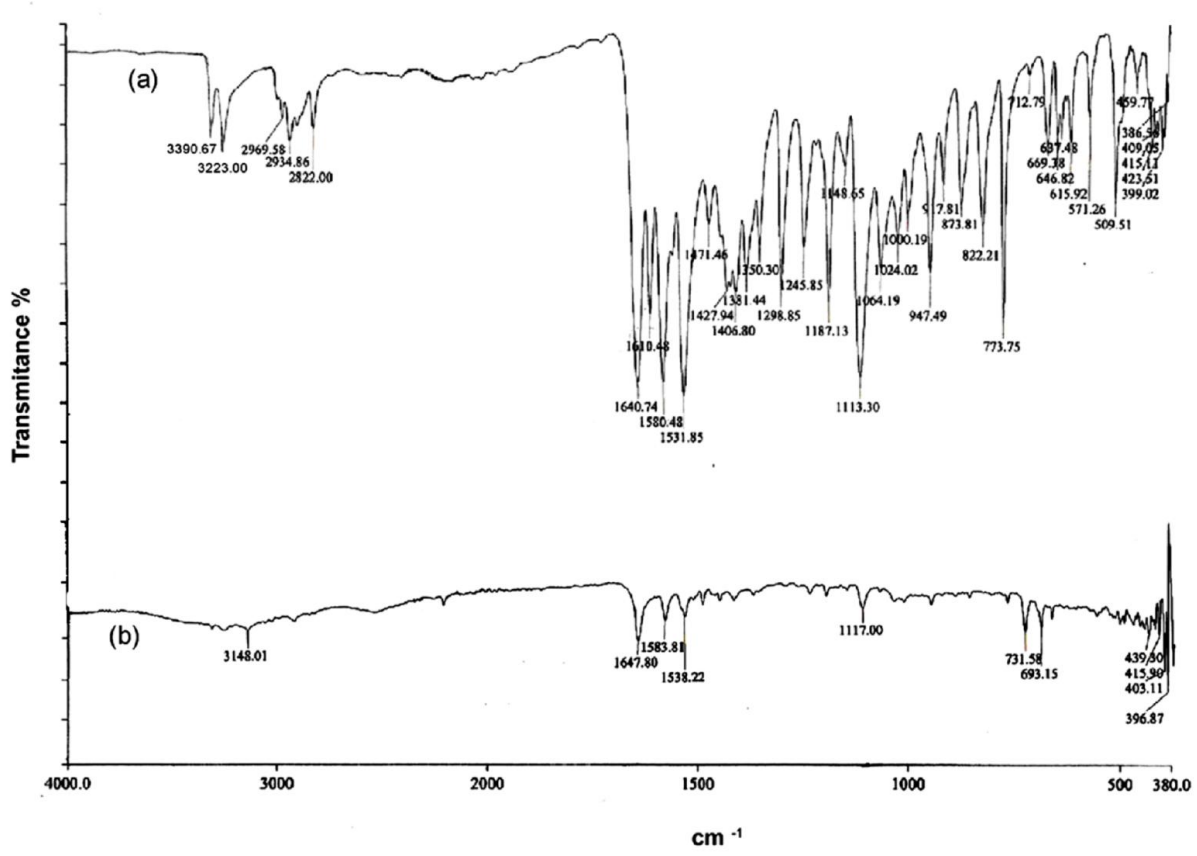

Figure 7. FTIR spectra (a) of compound B and (b) adsorption layer formed on the Al-3Mg alloy surface after immersion in 1 M HCl solution containing compound B ($c = 1\times10^{-4}$ M) for 3 h at 298 K.

The FTIR spectrum of adsorbed protective layer formed on Al-3Mg alloy surface after 3 h immersion in 1 M HCl containing compound B ($c = 1\times10^{-4}$ M) is shown in Fig. 7(b). This FTIR spectrum revealed that bands attributed to N–H and $–NH_2$ stretching vibrations become very weak is probably due to protonated amine [41] but also reveal the fact that compound B is adsorbed on the Al-3Mg alloy surface *via* nitrogen atoms in triazole ring. Moreover, the disappearance of the bands in the region from 1471 to 1363 cm^{-1} which are characteristic to C–H bending are also due the fact that compound B is protonated in acidic solutions.

Furthermore, in this FTIR spectrum can be observed changes in the shift of absorption bands caused by stretching frequency C=O group from1640 cm^{-1} to 1648 cm^{-1}, which indicates the bending with aluminium. This assumption is proven with appearance of two new absorption bands in the area from 731-693 cm^{-1} and band at 439 cm^{-1} which are characteristic for the vibrations of asymmetric and symmetric Al-O bending [45, 46]. Beside these, there is absorption band at 396 cm^{-1} which can be assigned to the Al–N stretching vibration [45]. Comparing Fig. 7(a) and (b), it can be suggested that

compound B can be adsorbed on the Al-3Mg alloy surface in cationic form and as neutral molecules. Previous studies confirmed the fact that in aqueous acidic solution the triazole molecules get protonated and exist either as neutral molecules or in the form of cations [47].

3.7. SEM examination

To investigate the performance of inhibitor, SEM study of Al-3Mg alloy samples was carried out after immersion in 1 M HCl solution for 3 h in the absence and presence of 1×10^{-4} M of compounds A and B (Fig. 8). Fig. 8a presented the SEM image for the non treated sample of Al-3Mg alloy. This micrograph is presented here for comparison with those of corroded samples. In this figure we can see some mechanical damage probably caused by cutting alloy in smaller pieces.

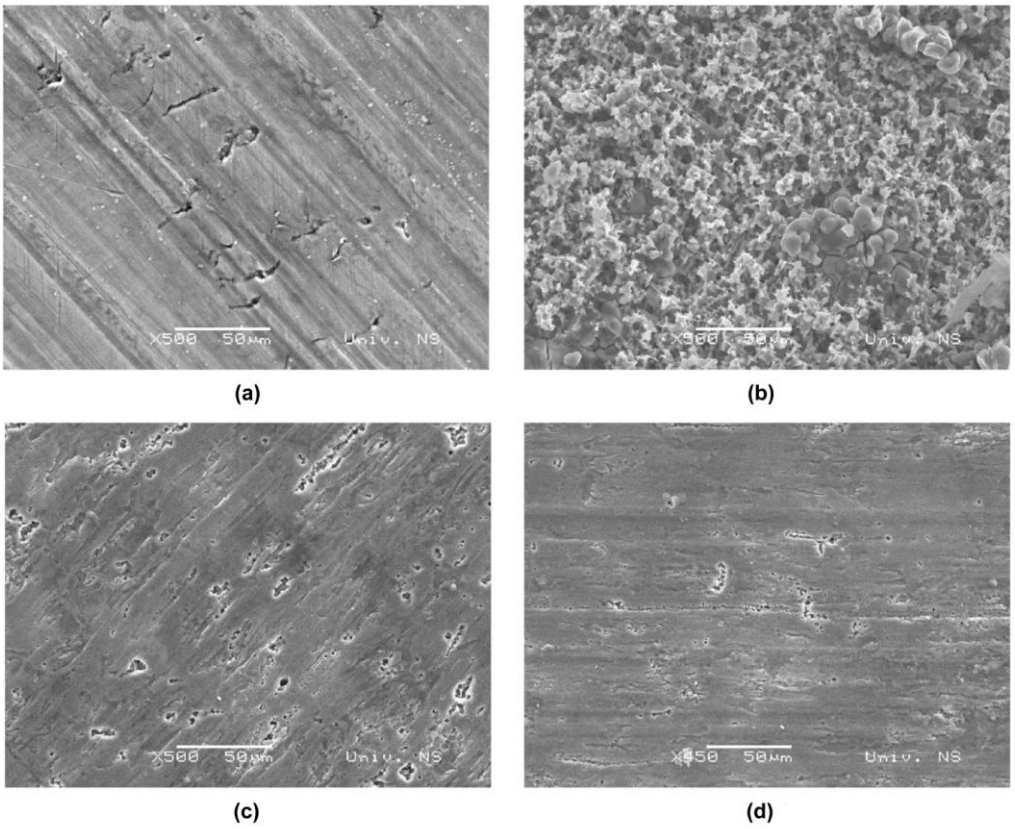

Figure 8. SEM images of the Al-3Mg alloy surface: (a) non treated sample, (b) after 3 h immersion in 1 M HCl solution, (c) after 3 h immersion in 1 M HCl solution in presence of compound A ($c = 1\times10^{-4}$ M) and (d) presence of compound B ($c = 1\times10^{-4}$ M).

The exposure of Al-3Mg alloy sample to 1 M HCl solution for 3 h, showed an aggressive attack of the corroding medium on the alloy surface, resulting mostly in general surface corrosion (Fig. 8b). By closer inspection, it became apparent that the corrosion was in the form of shallow pits covering the whole surface.

SEM images of samples immersed in 1 M HCl in presence of 1×10^{-4} M of compounds A and B are presented in Fig. 8c and 8d, showing improvements in surface morphology as compared to that in the chloride medium alone. Moreover, it is obvious, that on Al-3Mg alloy surface an adsorbed film of inhibitors is present. In accordance, it might be concluded that the adsorption film can efficiently inhibit the corrosion of Al-3Mg alloy. It was observed that, the number of pits for sample immersed in 1 M HCl in presence of 1×10^{-4} M of compound A (Fig. 8c) was slightly more pronounced and covered larger surface area than sample immersed in 1 M HCl in presence of 1×10^{-4} M of compound B (Fig. 8d). These results are in accordance with the results obtained by weight loss and polarization measurements.

3.8. Explanation for inhibition

On the basis of previous results the inhibition mechanism can be proposed. In general, owing to the complex nature of adsorption and inhibition of a given inhibitor, it is impossible to give exact adsorption mode between inhibitor and metal surface.

From all indications, the adsorption of compound A and compound B onto the Al-3Mg alloy surface involves two types of interactions: physisorption and chemisorption. In aqueous acidic solutions, the heterocyclic compounds investigated exist either as neutral molecules or in the form of cation (protonated species). As noted earlier, the proceeding of physical adsorption requires the presence of both, electrically charged surface of the metal and charged species in the bulk of the solution. From the literature [48] it is evident that aluminium surface is positively charged at pH 1, which is the pH value of HCl solutions that were used in this investigation. Therefore it is difficult for the protonated compounds to approach the positively charged Al-3Mg alloy surface due to the electrostatic repulsion. Since chloride ions have a smaller degree of hydration and being specifically adsorbed, they act as a bridge between the metal surface and the electrolyte [26, 48]. The protonated molecules of compounds investigated may adsorb through electrostatic interactions between the positively charged molecules and negatively charged metal surface, and there may be a synergism between chloride ions and protonated compounds.

Next explanation for mechanism of inhibition could be that, after these molecules are adsorbed on the aluminum surface by the electrostatic force, they may still react with aluminum to form the chemical bonds. Protonated species and neutral molecules can be adsorbed on the metal surface *via* the chemisorption mechanism, involving the coordinate type of bonds that can be formed between the lone electrons pairs of nitrogen and oxygen atoms and the empty p-orbitals of Al atoms on the surface of alloy investigated [49].

FTIR results reveal the fact that compound A can be adsorbed on the metal surface on the basis of donor-acceptor interactions between lone pair electrons of oxygen from carbonyl group and/or nitrogen atom carbonitrile group and vacant p-orbital of aluminium atom on the surface.

In addition, changes in FT-IR spectra support the interactions between functional groups of compound B and Al-3Mg alloy surface with assumption of bond *via* oxygen atom of carbonyl group and nitrogen atoms from 1,2,4- triazole ring. Recently, the molecular orbital calculations showed that

triazole compounds have more than one active center by which they would be adsorbed on the metal surface [50]. Therefore, for easily protonated compound B there are two ways to adsorption. First, it may be adsorbed via donor–acceptor interactions between the unshared electron pairs of the heteroatoms to form a bond with the vacant p-orbitals of the metal surface [51]. Second, in acidic media, $–NH_2$ group is readily protonated, which might adsorb onto the metallic surface *via* the negatively charge acid anions. Moreover, compound A may react with freshly generated Al^{3+} ions (firstly dissolved from the metal surface) forming Al- inhibitor complexes. These complexes might get adsorbed on Al-3Mg alloy surface due to electrostatic attraction effects to form an additionally protective layer leading to their high surface coverage and, hence, good corrosion inhibition [49]. This assumption is confirmed by the FTIR results.

On the other hand, the results show that compound B (triazole) is more efficient inhibitor, especially in 1 M HCl solution than compound A (pyridine derivative). This may be due to the higher molecular size and the presence of more nitrogen and oxygen atoms, which can act as additional adsorption centers and probable better protonation in acidic aqueous solution.

4. CONCLUSION

Compounds 4 - (methoxymethyl) - 1,6 – dimethyl – 2 – oxo-1,2-dihydropyridine-3-carbonitrile (compound A) and 4-amino-3,5-bis[6-(methoxymethyl)-3,4-dimethyl-2-oxo-1,2-dihydropyridine-1-yl]-1,2,4-triazole-2(*H*) (compound B) inhibit the corrosion of Al-3Mg alloy in 0.5 M and 1 M HCl at all concentrations used. The triazole derivative (compound B) is better inhibitor than pyridine derivative (compound A), what may be due to the higher molecular size and the presence of more nitrogen and oxygen atoms and probably better protonation in acidic media. Based on the results of polarization, both compounds act as mixed type inhibitors in 0.5 M and 1 M HCl solutions. On the basis of thermodynamic parameters and FTIR analysis it is obvious that the adsorption of compounds A and B involves two types of interactions: physisorption and chemisorption. The results suggest that the adsorption of inhibitor on Al-3Mg surface in both concentrations of HCl follows the Langmuir's adsorption isotherm. FTIR results reveal that compound A can be adsorbed on the metal surface on the basis of donor-acceptor interactions between lone pair electrons of oxygen from carbonyl group and/or nitrogen atom carbonitrile group and vacant p-orbital of aluminium atom on the surface. In addition, changes in FTIR spectra support the interactions between functional groups of compound B and Al-3Mg alloy surface with assumption of bond *via* oxygen atom of carbonyl group and nitrogen atoms from 1,2,4- triazole ring.

ACKNOWLEDGEMENTS

The financial support of the Ministry of Science, Technology and Sport of Republic of Croatia (Grant No. 058-0582261-2253 and 058-0582261-2256) is gratefully acknowledged. Special recognition goes to Prof. M. Gojo (Faculty of Graphic Arts, University of Zagreb) for helpful discussions and M. Bokorov (University of Novi Sad) for the SEM work. The efficient assistance of A. Katović (Faculty

of Textile Technology, University of Zagreb) for FT-IR spectroscopy is greatly acknowledged. This paper is based on a part of the dissertation work of J. Halambek.

References

1. S.M.A. Hosseini, M. Salari, E. Jamalizadeh, S. Khezripoor, M. Seifi, *Mater. Chem. Phys*., 119 (2010) 100.
2. A.K. Maayta, N.A.F. Al-Rawashdeh, *Corros. Sc.*, 46 (2004) 1129.
3. N. O. Eddy, E. E. Ebenso, *Int. J. Electrochem. Sci*., 5 (2010) 731.
4. N.O. Obi-Egbedi, K.E. Essien, I.B. Obot, E.E. Ebenso, *Int. J. Electrochem. Sci*., 6 (2011) 913.
5. Jiajun Fu, Junyi Pan, Zhuo Liu, Suning Li1, Ying Wang, *Int. J. Electrochem. Sci.*, 6 (2011) 2072.
6. K.F. Khaled, M.M. Al-Qahtani, *Mater. Chem. Phys*., 113 (2009) 150.
7. Q.B. Zhang, Y.X. Hua, *Mater. Chem. Phys.*, 119 (2010) 57.
8. I.B. Obot, N.O. Obi-Egbedi, S.A. Umoren, *Corros. Sci.*, 51 (2009) 1868.
9. G. Schmitt, *Br. Corros. J.*, 19 (1984) 165.
10. S.A. Abd El-Maksoud, A.S. Fouda, *Mater. Chem. Phys.*, 93 (2005) 84.

A. Chetouani, K. Medjahed, K.E. Sid-Lakhdar, B. Hammouti, M. Benkaddour, A. Mansri, *Corros. Sci.*, 46 (2004) 2421.

11. M. Lashkari, M.R. Arshadi, *Mater. Chem. Phys.*, 299 (2004) 131.
12. Y. Xiao-Ci, Z. Hong, L. Ming-Dao, R. Hong-Xuan, Y. Lu-An, *Corros. Sci*., 42 (2000) 645.
13. S. Ramesh, S. Rajeswari, *Electrochim. Acta*, 49 (2004) 811.
14. H. H. Hassan, E. Abdelghani, M. A. Amin, *Electrochim. Acta*, 52 (2007) 6359.
15. F. Xu, J. Duan, S. Zhang, B. Hou, *Mater. Lett.*, 62 (2008) 4072.
16. A.K. Satpati , P.V. Ravindran, *Mater. Chem. Phys*., 109 (2008) 352.
17. M.L. Zheludkevich, K.A. Yasakau, S.K. Poznyak, M.G.S. Ferreira, *Corros. Sci.*, 47 (2005) 3368.
18. M. Cetina, M. Tranfić, I. Sviben, M. Jukić, *J. Mol. Struct*., 969 (2010) 25.
19. M. Jukić, M. Cetina, J. Halambek, I. Ugarković, *J. Mol. Struct.*, 979 (2010) 108.
20. K. Matsukawa, J. Setsune, K. Takagi, T. Kitao, *Dyes Pigments*, 3 (1982) 307.
21. F. Bentiss, M. Lagrenée, M. Traisnel, B. Mernari, H. Elattari, *J. Heterocyclic Chem*., 36 (1999) 149.
22. F. Bentiss, M. Lagrenée, D. Barbry, *Tetrahedron Lett.*, 41 (2000) 1539.
23. F. Bentiss, M. Bouanis, B. Mernari, M. Traisnel, H. Vezin, M. Lagrenee, *Appl. Surf. Sci.*, 253 (2007) 3696.
24. L. Herrag, B. Hammouti, S. Elkadiri, A. Aounit, C. Jama, H. Vezin, F. Bentiss, *Corros. Sci.*, 52 (2010) 3042.
25. A.Yurt, S. Ulutas, H. Dal, *Appl. Surf. Sci*., 253 (2006) 919.
26. K.C. Emregul, O. Atakol, *Mater. Chem. Phys.*, 83 (2004) 373.
27. K.S. Jacob, G. Parameswaran, *Corros. Sci.*, 52 (2010) 224.
28. F.S. de Souza, A. Spinelli, *Corros. Sci.*, 51 (2009) 642.
29. A.Popova, M. Christov, A. Vasilev, A. Zwetanova, *Corros. Sci*., 53 (2011) 679.
30. A.Y. Musa, A.A. H. Kadhum, A.B. Mohamad , M.S. Takriff, A. R. Daud, S. K. Kamarudin, *Corros. Sci*., 52 (2010) 526.
31. E.E. Ebenso, I. B. Obot, L. C. Murulana, *Int. J. Electrochem. Sci.*, 5 (2010**)** 1574.
32. E. A. Noor, A.H. Al-Moubaraki, *Mater. Chem. Phys*., 110 (2008) 145.
33. M. Lagrenee, B.Mernari, M. Bouanis, T. Traisnel, F. Bentiss, *Corros. Sci.*, 44 (2002) 573.
34. F. Bentiss, M. Lebrini, M. Lagrenee, *Corros. Sci.*, 47 (2005) 2915.
35. I.Ahamad, R. Prasad, M.A. Quraishi, *Corros. Sci.*, 52 (2010) 3033.
36. A.Popova, *Corros. Sci.*, 49 (2007) 2144.
37. A.Y. El-Etre, *J. Colloid Interf. Sci.*, 314 (2007) 578.

38. O.K. Abiola, A.O. James, *Corros. Sci.*, 52 (2010) 661.
39. A.Popova, E. Sokolova, S. Raicheva, M. Christov, *Corros. Sci.*, 45 (2003) 331.
40. Q. Qu, S. Jiang, W. Bai, L. Li, *Electrochim. Acta*, 52 (2007) 6811.
41. M. J. Bahrami, S.M.A. Hosseini, P. Pilvar, *Corros. Sci.*, 52 (2010) 2793.
42. S. A. Umoren, Y. Li, F.H. Wang, *J. Solid. State. Electrochem.*, 14 (12), (2010) 2293.
43. R.J. Moolenaar, J.C. Evans, L.D. McKeever, *J Phys. Chem*., 74 (1970) 3629.
44. P.S. Kalsi, Spectroscopy of Organic Compounds, New Age International Publishers, New Delhi, 2004.
45. G. Socrates, Infrared and Raman Characteristic Group Frequencies, John Wiley and Sons, 2004.
46. J.O.M. Bockris, B. Yang, *J. Electrochem.*, 12 (1996) 853.
47. I.B. Obot, N.O. Obi-Egbedi, *Colloid Surface A*, 330 (2008) 207.
48. X.Li, S. Deng, H. Fu, *Corros. Sci.*, 53 (2010) 1529.
49. M.K. Awad, M.R. Mustafa, M.M. Abo Elnga, *J. Mol. Struct:THEOCH.*, 959 (2010) 66.
50. G. Y. Elewady, *Int. J. Electrochem. Sci.*, 3 (2008) 1149.